中国物理 B
Chinese Physics
Chinese Physics B

Quaternary antiferromagnetic Ba_2BiFeS_5 with isolated FeS_4 tetrahedra

Shaohua Wang(王少华), Xiao Zhang(张晓), Hechang Lei(雷和畅)
Citation: Chin. Phys. B, 2019, 28 (**8**): 087401 **doi:** 10.1088/1674-1056/28/8/087401
Journal homepage: http://cpb.iphy.ac.cn; http://iopscience.iop.org/cpb

What follows is a list of articles you may be interested in

0-π transition induced by the barrier strength in spin superconductor Josephson junctions

Wen Zeng(曾文), Rui Shen(沈瑞)
Chin. Phys. B . 2018, 27(9): 097401 . **doi:** 10.1088/1674-1056/27/9/097401

Superconducting quantum bits

Wei-Yang Liu(刘伟洋), Dong-Ning Zheng(郑东宁), Shi-Ping Zhao(赵士平)
Chin. Phys. B . 2018, 27(2): 027401 . **doi:** 10.1088/1674-1056/27/2/027401

Validation of the Wiedemann-Franz law in a granular s-wave superconductor in the nanometer scale

A Yousefvand, H Salehi, M Zargar Shoushtari
Chin. Phys. B . 2017, 26(3): 037401 . **doi:** 10.1088/1674-1056/26/3/037401

Novel 0-π transitions in Josephson junctions between noncentrosymmetric superconductors

Jun-Feng Liu(刘军丰), Huan Zhang(张欢), Jun Wang(汪军)
Chin. Phys. B . 2016, 25(9): 097403 . **doi:** 10.1088/1674-1056/25/9/097403

Retrieval of original signals for superconducting quantum interference device operating in flux locked mode

Liu Dang-Ting, Tian Ye, Zhao Shi-Ping, Ren Yu-Feng, Chen Geng-Hua
Chin. Phys. B . 2015, 24(4): 047402 . **doi:** 10.1088/1674-1056/24/4/047402

Quaternary antiferromagnetic Ba_2BiFeS_5 with isolated FeS_4 tetrahedra

Shaohua Wang(王少华)[1], Xiao Zhang(张晓)[2], and Hechang Lei(雷和畅)[1,†]

[1] *Department of Physics and Beijing Key Laboratory of Opto-electronic Functional Materials & Micro-nano Devices, Renmin University of China, Beijing* 100872, *China*

[2] *State Key Laboratory of Information Photonics and Optical Communications & School of Science, Beijing University of Posts and Telecommunications, Beijing* 100876, *China*

(Received 12 May 2019; revised manuscript received 6 June 2019; published online 25 July 2019)

We report the detailed physical properties of quaternary compound Ba_2BiFeS_5 with the key structural ingredient of isolated FeS_4 tetrahedra. Magnetization and heat capacity measurements clearly indicate that Ba_2BiFeS_5 has a paramagnetic to antiferromagnetic transition at about 30 K. The calculated magnetic entropy above ordering temperature is much smaller than theoretical value for high-spin Fe^{3+} ion with $S = 5/2$, implying the possible short-range antiferromagnetic fluctuation in Ba_2BiFeS_5.

Keywords: isolated FeS_4 tetrahedra, antiferromagnetic transition, short-range antiferromagnetic fluctuation

PACS: 74.50.+r, 75.20.Ck, 75.30.–m, 75.30.Cr **DOI:** 10.1088/1674-1056/28/8/087401

1. Introduction

The discovery of iron-based superconductors promotes the development of studies on iron-based materials.[1–6] In the past decade, different kinds of iron-based compounds are reported and they can be classified according to the dimensionality of structural unit formed by the FeX_4 (X = pnictogens and chalcogens) tetrahedra. Most of iron-based superconductors, such as LaOFeAs, $BaFe_2As_2$, FeSe, $(Li_{1-x}Fe_x)$OHFeSe, and $Li_x(NH_3)_yFe_2Se_2$,[1,2,6–9] share common two-dimensional (2D) FeX layers built up with edge-sharing FeX_4 tetrahedra.[10] When FeX_4 tetrahedra connect each other along one crystallographic axis via edge sharing, they can form quasi-one-dimensional (quasi-1D) compounds such as $KFeS_2$ with single 1D FeS_4 chain along the c axis,[11] $BaFe_2S_3$ and $BaFe_2Se_3$ with double 1D FeS_4 or $FeSe_4$ chains (spin-ladder structure) along the b axis.[12–14] The latter compounds exhibit Mott insulating behaviors with antiferromagnetic (AFM) orders at ambient pressure.[12–14] Interestingly, both of $BaFe_2S_3$ and $BaFe_2Se_3$ show superconductivity under pressure.[15–17] Moreover, the connected edge-sharing FeX_4 tetrahedra can also form three-dimensional (3D) compounds like $CaFe_4As_3$.[18] It displays non-Fermi-liquid behavior at zero field with enhanced electron–electron correlations.[18] Thus, exploration of iron-based compounds with various dimensionality of FeX_4 units would provide a comprehensive understanding of the relation between electronic correlation and dimensionality in the iron-based materials.

When compared to the extensively studied ternary compounds, the studies on quaternary iron-based compounds are still rare so far. Recently, the quaternary compounds $Ba_2PnFeCh_5$ (Pn = Sb, Bi, and Ch = S, Se) containing isolated (zero-dimensional, 0D) $FeCh_4$ tetrahedra are reported.[19–21] Previous studies indicate that they exhibit AFM order at low temperature in general.[19–21] In this work, we have grown the single crystal of Ba_2BiFeS_5 and carried out a detailed study on physical properties. It shows a long-range AFM order with Neel temperature $T_N \sim 30$ K, and there may be an AFM fluctuation before the formation of longe-range antiferromagnetism.

2. Experiment

Single crystals of Ba_2BiFeS_5 were grown by solid state reaction method. Ba pieces (99.9%), Bi shots (99.99%), Fe lumps (99.98%), and S granules (99.999%) were mixed with a stoichiometric molar ratio Ba:Bi:Fe:S = 2:1:1:5. The mixture was loaded in an alumina crucible which was put into a quartz tube. These operations were handled in the glovebox with the O_2 and H_2O contents under 0.1 ppm. Then the quartz tube was sealed with Ar gas under the pressure of 0.2 atmospheres. The sealed tube was heated up to 1273 K for 24 h and kept at 1273 K for 48 h. Then it was cooled down to 673 K with 3 K/h before finally switching off the furnace. The crystals can be extracted from the matrix mechanically. X-ray diffraction (XRD) patterns were collected using a Bruker D8 X-ray Diffractometer with Cu K_α radiation (λ = 1.5418 Å) at room temperature. The lattice pa-

*Project supported by the National Key Research and Development Program of China (Grant No. 2016YFA0300504), the National Natural Science Foundation of China (Grant Nos. 11574394, 11774423, and 11822412), the Fundamental Research Funds for the Central Universities, and the Research Funds of Renmin University of China (RUC) (Grant Nos. 15XNLQ07, 18XNLG14, and 19XNLG17).

†Corresponding author. E-mail: hlei@ruc.edu.cn

© 2019 Chinese Physical Society and IOP Publishing Ltd

rameters were obtained by fitting the powder XRD pattern using the TOPAS4 software.[22] The elemental analysis was performed using an energy-dispersive x-ray spectroscopy (EDX) in a JEOL JSM-6500 scanning electron microscope. Magnetization measurements were performed in a Quantum Design Magnetic Property Measurement System (MPMS3). Heat capacity measurements were performed in Quantum Design PPMS-14.

3. Results and discussion

Figure 1(a) shows the structure of Ba_2BiFeS_5. The structure is formed by alternatively stacking Fe–Bi–S layers and Ba^{2+} cations along the *a* axis. The main building blocks of a Fe–Bi–S layer in the *bc* plane are FeS_4 tetrahedra and BiS_5 quadrangular pyramids. As shown in Fig. 1(b), the 1D connected chain of BiS_5 along the *b* axis consists of edge-sharing BiS_5 quadrangular pyramids. Via edge sharing, FeS_4 tetrahedra connect on both sides of this chain along the *c* axis alternatively with the atomic distance $d_{Fe-Bi} = 3.264$ Å. On the other hand, the shortest atomic distance between two Fe ions in the neighboring Fe–Bi–S chains is very large (∼ 5.8 Å), comparable with the interchain distance of Fe ions in $BaFe_2S_3$ (∼ 5.86 Å).[12] Thus, FeS_4 tetrahedron in Ba_2BiFeS_5 can be viewed as a 0D unit. Figure 1(c) shows the powder x-ray diffraction pattern of the ground crystals and it is found that this pattern can be well fitted by the Rietveld method using the reported structure of Ba_2BiFeS_5 (space group *Pnma*) with minor second phase $BaBi_2S_4$ (∼ 6.9(1) wt%). It is hard to eliminate the minority phase of $BaBi_2S_4$ because it is very stable and its formation temperature overlaps with Ba_2BiFeS_5.[23] The refined lattice parameters are $a = 12.1378(7)$ Å, $b = 8.9419(4)$ Å, and $c = 8.8294(5)$ Å. These values are close to previous results[19] but slightly smaller than those in $Ba_2BiFeSe_5$,[20,21] which can be ascribed to the smaller ionic size of S than Se. The analysis of EDX result shown in Fig. 1(d) confirms the existence of Ba, Bi, Fe, and S. The obtained ratio of Ba:Bi:Fe:S is 2.17(3):0.99(6):1:5.34(3) when setting the content of Fe as 1, consistent with the chemical formula of Ba_2BiFeS_5. The inset of Fig. 1(d) displays the photograph of typical crystals of Ba_2BiFeS_5. They have a sub-millimeter size with black color. The subquadrate shape is in agreement with the crystallographic symmetry of Ba_2BiFeS_5.

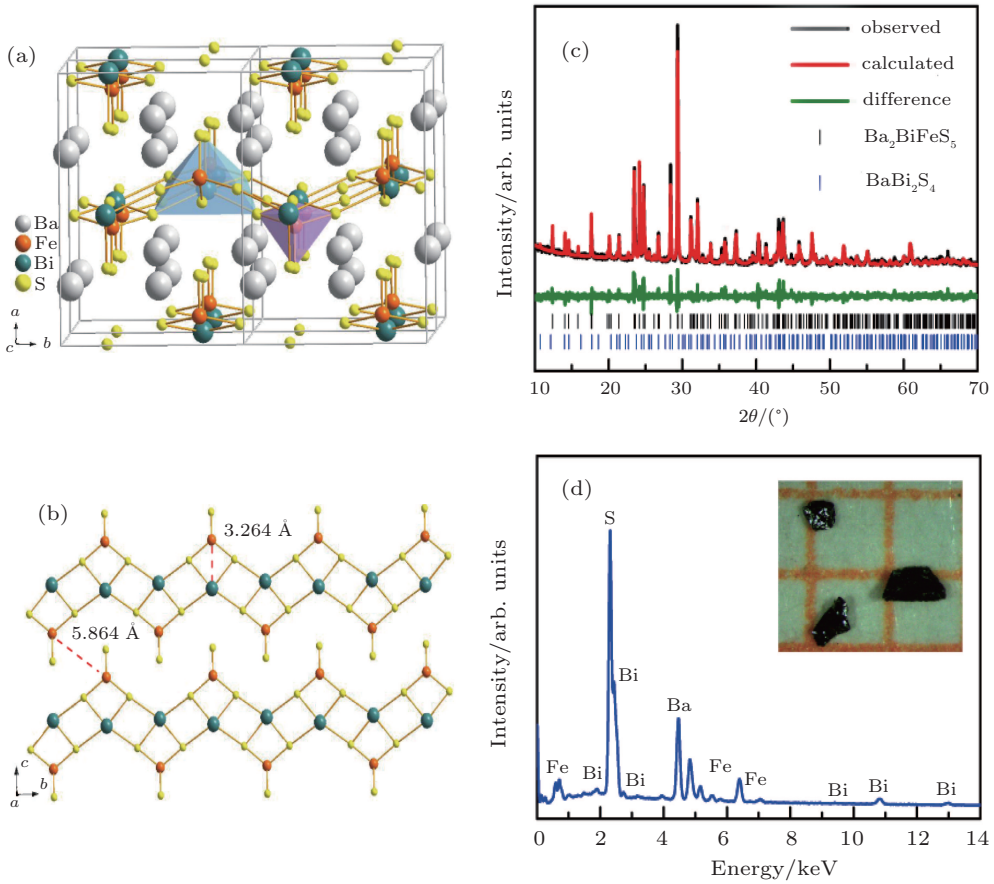


Fig. 1. (a) Crystal structure of Ba_2BiFeS_5. The white, orange, dark green, and yellow balls represent Ba, Fe, Bi, and S atoms, respectively. (b) Structural unit of an infinite $^{\infty}_{1}[FeBiS]^{4-}$ chain arranged in the *bc* plane. The shortest atomic distances of intrachain Fe–Bi and interchain Fe–Fe are marked. (c) Powder XRD pattern of crushed Ba_2BiFeS_5 single crystals. The black and red line represents the observed and calculated pattern, respectively, and the green line shows the difference between them. The black and blue bars represent the peak portions of Ba_2BiFeS_5 and the minor second phase $BaBi_2S_4$, respectively. (d) The EDX spectrum of Ba_2BiFeS_5 single crystal. Inset: photo of obtained Ba_2BiFeS_5 single crystals. The length of one grid in the photo is 1 mm.

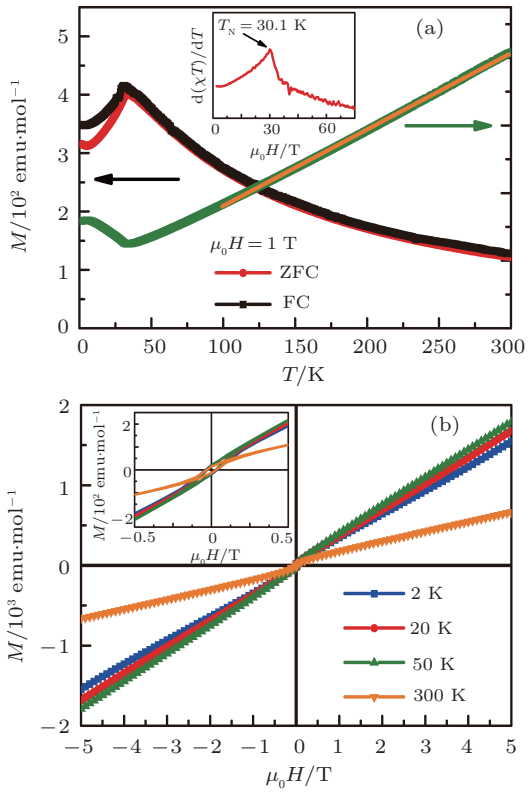


Fig. 2. (a) Temperature dependence of magnetization $M(T)$ from 1.8 K to 300 K with the zero-field cooling (ZFC) and the field cooling (FC) modes and the Curie–Weiss fitting of temperature dependence of inverse magnetic susceptibility $1/\chi(T)$ (orange solid line). Inset: $\mathrm{d}(\chi T)/\mathrm{d}T$ as a function of T. (b) Isothermal magnetization hysteresis loops $M(\mu_0 H)$ in the field range from −5 T to 5 T at various temperatures. Inset: the enlarged part of $M(\mu_0 H)$ curves at low-field region.

Temperature dependence of magnetization $M(T)$ for several pieces of Ba_2BiFeS_5 crystals at $\mu_0 H = 1$ T is shown in Fig. 2(a). It can be seen that the $M(T)$ increases as the temperature decreases from 300 K to 35 K. There is a sudden drop when lowering temperature further, suggesting that there is an AFM transition in Ba_2BiFeS_5. The determined AFM transition temperature T_N from the peak of $\mathrm{d}(\chi T)/\mathrm{d}T$ curve with zero-field cooling mode is 30.1 K (the inset of Fig. 2(a)),[24] which is consistent with the pervious report.[19] When $T < T_N$, there is a similar drop in the field-cooling (FC) $M(T)$ curve, implying the absence of magnetic glassy state. When $T < 6$ K, there are upturns appearing in both ZFC and FC $M(T)$ curves, possibly due to the contribution of minor impurities in the sample. For $T > T_N$, the inverse of magnetic susceptibility $1/\chi(T)$ exhibits the nearly linear behavior up to 300 K (Fig. 2(a)). It can be fitted very well using the Curie–Weiss law $\chi(T) = C/(T-\theta)$, where C is the Curie constant and θ is the Weiss temperature. The linear fit of $1/\chi(T)$ between 100 K and 300 K with ZFC mode (orange solid line in Fig. 2(a)) gives $C = 4.42(5)$ emu $\cdot$ g^{-1} $\cdot$ Oe^{-1} $\cdot$ K and $\theta = -60.27(6)$ K, indicating the dominant AFM interaction in this material. It is also in agreement with the AFM ordering below T_N. The value of C corresponds to the effective moment $\mu_{\mathrm{eff}} = 5.94(3)$ μ_B/Fe, close to the expected local moment of high-spin Fe^{3+} ion ($S = 5/2$, spin-only $\mu_{\mathrm{eff}} = 5.92$ μ_B/Fe). Compared to isostructural $Ba_2BiFeSe_5$ with larger $T_N \sim 79$ K, the shortest Fe–Fe distance in Ba_2BiFeS_5 (5.864 Å) is shorter than that in $Ba_2BiFeSe_5$ (6.0 Å),[21] indicating the direct magnetic interactions may not be dominant. Meanwhile, band structure calculations show that Ba_2BiFeS_5 is an insulator with no conduction electron,[19] so that the RKKY interaction is excluded. Thus one of the possible magnetic interacting mechanisms is superexchanging interaction, *i.e.*, Fe atoms interact with each other via Bi and/or S atoms.[21] Figure 2(b) shows the field dependence of magnetization $M(H)$ at various temperatures. The $M(H)$ loops exhibit the almost linear behaviors without the trend of saturation, irrespective of temperatures, consistent with the feature of AFM transition in Ba_2BiFeS_5. It has to be noted that there is a small hysteresis at low-field region for all of curves, even when $T > T_N$. This could originate from the minor ferromagnetic impurities in the sample.

The specific heat capacity $C_p(T)$ measurement from 2 K to 150 K is presented in Fig. 3(a). An anomalous behavior can be obviously observed at 31.3 K, corresponding to the long-range AFM transition. The T_N obtained from the peak in $C_p(T)$ curve is close to that derived from the $\mathrm{d}(\chi T)/\mathrm{d}T$ curve in the inset of Fig. 2(a). Because of the AFM insulator feature of Ba_2BiFeS_5,[19] the total specific heat capacity can be divided into lattice (C_{ph}) and magnetic (C_m) parts. The C_{ph} can be fitted using the 5th polynomial between temperature range of 2 K–10 K and 70 K–100 K (red solid line in Fig. 3(a)). This method has been adopted in previous reports to estimate the heat capacity of lattice vibration.[25–27] After subtracting the lattice contribution, the obtained $C_m(T)$ is presented in Fig. 3(b) (green symbols). There is a peak shown in $C_m(T)$ curve, corresponding to the paramagnetic (PM) to AFM transition.

Magnetic entropy $S_m(T)$ can be calculated by integrating the C_m/T. The derived temperature dependence of $S_m(T)$ is shown in Fig. 3(b)(orange solid line). It can be seen that the $S_m(T)$ is small when T is far below T_N. However, it increases dramatically when T is approaching T_N because of the significant release of magnetic entropy at PM–AFM traction. Finally, it becomes saturated at higher temperature. The value of S_m at 100 K is 6.6 J $\cdot$ mol^{-1} $\cdot$ K^{-1}, which is much smaller than theoretical value $R\ln(2S+1) = 14.9$ J $\cdot$ mol^{-1} $\cdot$ K^{-1} for high-spin Fe^{3+} ion with $S = 5/2$ (brown dashed line, Fig. 3(b)). One of the possible reasons is the existing of short range magnetic fluctuation above T_N, partially reflecting from the difference between the θ and T_N. The overestimation of C_{ph} would be another reason causing the smaller values of C_m and corresponding S_m than actual ones. On the other hand, assuming the neglible contribution of $C_m(T)$ at low temperature

($T < 10$ K), the $C_p(T)$ can be well fitted using the formula $C_p/T = \beta T^2$ (inset of Fig. 3(a)). The value of coefficient related to the phonon contribution β is 4.85(9) mJ · mol^{-1} · K^{-4} and the calculated Debye temperature is $\Theta_D = 153(3)$ K using the formula $\Theta_D = (12\pi^4 NR/5\beta)^{1/3}$, where N is the atomic number in the chemical formula ($N = 9$) and R is the gas constant ($R = 8.314$ J · mol^{-1}K^{-1}). It should be noted that the derived Θ_D from fitted β has some uncertainty because the temperature dependence of heat capacity for antiferromagnetic magnons excitation also follow the T^3 behavior.

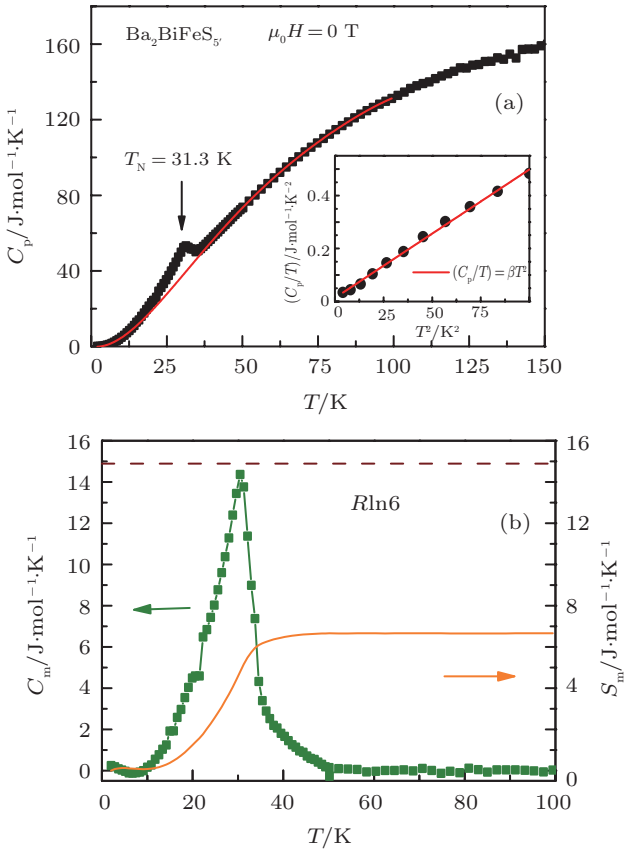


Fig. 3. (a) Temperature dependence of heat capacity $C_p(T)$ for Ba_2BiFeS_5 single crystal at zero field. The red solid curve represents the lattice contribution, fitted by a polynomial. Inset: enlarged part at low temperature region. The red solid line is the fit using the formula $C_p(T)/T = \beta T^2$. (b) Temperature dependence of $C_m(T)$ (left label, green symbols) and $S_m(T)$ curves (right label, orange solid line). The brown dashed line represents the theoretical value of S_m ($R\ln 6$ for $S = 5/2$ system).

4. Conclusion

In summary, we grew single crystal of Ba_2BiFeS_5 containing 0D structural unit of FeS_4 tetrahedra. The fit of high-temperature $M(T)$ curve using the Curie–Weiss law gives the $\mu_{eff} = 5.94(3)$ μ_B/Fe, indicating that the Fe^{3+} ions in this compound are at the high-spin state ($S = 5/2$). Moreover, the negative value of θ (~ -60 K) suggests the dominant AFM interaction. The long-range AFM order forms at $T_N \sim 30$ K, confirmed by both magnetization and heat capacity measurements. By analyzing the $C_m(T)$, we find that the S_m at T_N (4.79 J · mol^{-1} K^{-1}) is much smaller than the theoretical value for high-spin state Fe^{3+} ions (14.9 J · mol−1 · K^{-1}). It might be ascribed to the short-range antiferromagnetic fluctuation above T_N or the overestimated phonon contribution to heat capacity.

References

[1] Kamihara Y, Watanabe T, Hirano M and Hosono H 2008 *J. Am. Chem. Soc.* **130** 3296

[2] Hsu F C, Luo J Y, Yeh K W, Chen T K, Huang T W, Wu P M, Lee Y C, Huang Y L, Chu Y Y, Yan D C and Wu M K 2008 *Proc. Natl. Acad. Sci. USA* **105** 14262

[3] Rotter M, Tegel M and Johrendt D 2008 *Phys. Rev. Lett.* **101** 107006

[4] Sasmal K, Lv B, Lorenz B, Guloy A M, Chen F, Xue Y Y and Chu C W 2008 *Phys. Rev. Lett.* **101** 107007

[5] Mizuguchi Y, Tomioka F, Tsuda S, Yamaguchi T and Takano Y 2008 *Appl. Phys. Lett.* **93** 152505

[6] Tapp J H, Tang Z J, Lv B, Sasmal K, Lorenz B, Chu P C W and Guloy A M 2008 *Phys. Rev. B* **78** 060505

[7] Ying T P, Chen X L, Wang G, Jin S F, Zhou T T, Lai X F, Zhang H and Wang W Y 2012 *Sci. Rep.* **2** 426

[8] Lu X F, Wang N Z, Wu H, Wu Y P, Zhao D, Zeng X Z, Luo X G, Wu T, Bao W, Zhang G H, Huang F Q, Huang Q Z and Chen X H 2015 *Nat. Mater.* **14** 325

[9] Burrard-Lucas M, Free D G, Sedlmaier S J, Wright J D, Cassidy S J, Hara Y, Corkett A J, Lancaster T, Baker P J, Blundell S J and Clarke S J 2013 *Nat. Mater.* **12** 15

[10] Chen X H, Dai P H, Feng D L, Xiang T and Zhang F C 2014 *Natl. Sci. Rev.* **1** 371

[11] Bronger W, Kyas A and Muller P 1987 *J Solid State Chem* **70** 262

[12] Serpil Gonen Z, Fournier P, Smolyaninova V, Greene R, Araujo-Moreira F M and Eichhorn B 2000 *Chem. Mater.* **12** 3331

[13] Lei H C, Ryu H, Frenkel A I and Petrovic C 2011 *Phys. Rev. B* **84** 214511

[14] Caron J M, Neilson J R, Miller D C, Llobet A and McQueen T M 2011 *Phys. Rev. B* **84** 180409

[15] Takahashi H, Sugimoto A, Nambu Y, Yamauchi T, Hirata Y, Kawakami T, Avdeev M, Matsubayashi K, Du F, Kawashima C, Soeda H, Nakano S, Uwatoko Y, Ueda Y, Sato T J and Ohgushi K 2015 *Nat. Mater.* **14** 1008

[16] Yamauchi T, Hirata Y, Ueda Y and Ohgushi K 2015 *Phys. Rev. Lett.* **115** 246402

[17] Ying J J, Lei H C, Petrovic C, Xiao Y M and Struzhkin V V 2017 *Phys. Rev. B* **95** 241109

[18] Karki A B, McCandless G T, Stadler S, Xiong Y M, Li J, Chan J Y and Jin R 2011 *Phys. Rev. B* **84** 054412

[19] Geng L, Cheng W D, Zhang H, Lin C S, Zhang W L, Li Y Y and He Z Z 2011 *Inorg. Chem.* **50** 2378

[20] Li X S, Zhang X, Kalai Selvan G, Arumugam S, Huang F Q, Wu Y C and Yao J Y 2016 *Chem. Asian J.* **11** 3436

[21] Wang J, Greenfield J T and Kovnir K 2016 *J. Solid State Chem.* **242** 22

[22] TOPAS Version 4.2; 2009 Bruker AXS, Karlsruhe, Germany

[23] Aurivillius B 1983 *Acta Chem. Scand. A* **37** 399

[24] Fisher M E 1962 *Philos. Mag.* **7** 1731

[25] Zhou C S, Wang J F, Liu X, Chen F Y, Di Y Y, Gao S L and Shi Q 2018 *New J. Chem.* **42** 8400

[26] Gupta S, Das A, Suresh K G, Hoser A, Knyazev Y V, Kuzmin Y I and Lukoyanov A V 2015 *Mater. Res. Exp.* **2** 046101

[27] Loos S, Gruner D, Abdel-Hafiez M, Seidel J, Hüttl R, Wolter A, Bohmhammel K and Mertens F 2015 *J. Chem. Thermodyn.* **85** 77